Applied Acoustics 216 (2024) 109830

Contents lists available at ScienceDirect

Applied Acoustics

journal homepage: www.elsevier.com/locate/apacoust

Numerical model for vibro-acoustics analysis of tyre-road noise generation caused by speed bumps

Miguel Fabra-Rodriguez *, David Abellán-López, Francisco J. Simón-Portillo, Hector Campello-Vicente, Nuria Campillo-Davo, Ramon Peral-Orts

Miguel Hernández University of Elche, Avda. de la Universidad, s/n, 03202 Elche, (Alicante), Spain

ARTICLE INFO

Keywords:
Rolling noise
Impact noise
FEM-BEM Modelling
Speed bump

ABSTRACT

Electric vehicles, particularly when driving at low speeds, present a solution to mitigate the impact of road traffic on noise pollution. However, specific urban traffic scenarios still give rise to increased noise levels due to road irregularities such as speed bumps. To address this issue, a model that combines a dynamic analysis using FEM with an acoustic analysis using BEM is developed. The dynamic analysis simulates a quarter vehicle, employing a 3D tyre model equipped with a suspension system, to replicate impacts against obstacles. The resulting tyre vibration serves as a sound source for the study of acoustic propagation. To validate this model, low-speed track tests were conducted using an electric vehicle driving over a speed bump. The instrumentation used was an acoustic camera, which allowed the evaluation of the sound pressure level reached during the tests.

1. Introduction

Environmental noise is a serious problem in Europe. At least 20 % of its population lives in areas where traffic noise levels are detrimental to health. It is estimated that 113 million people are exposed to prolonged noise levels of at least 55 *dB(A)* due to this cause [1]. Exposure to such high noise levels can cause a variety of ailments such as sleep disorders [2,3], learning disorders [3] or hypertension [4].

It is therefore necessary to study and analyse the characteristics of the different noise generation mechanisms of a vehicle as a noise source: the mechanical noise of the propulsion system, aerodynamic noise and tyre-road interaction noise [5]. Depending on the driving speeds, each of these sources contributes differently to total noise emission [6]. In urban areas, where most of the population affected by noise pollution lives, low driving speeds make the contribution of aerodynamic noise negligible. On the other hand, noise contribution from the engine and propulsion systems of conventional vehicles predominates at speeds below 30 *km/h*, while tyre-road noise prevails at speeds above that value [6].

Technological advances and the implementation of new regulations has led to a gradual reduction in vehicle noise emissions over time [7]. However, the electrification of vehicles has led to a drastic reduction in the noise generated by their propulsion systems [8], leaving tyre-road interaction as the main noise source in urban areas. Therefore, it is of particular interest to take a closer look at the different phenomena that constitute the noise generated by tyre-road interaction. The phenomena can be divided into two groups [6]: the aerodynamics of the emission zone and mechanical vibrations. On the one hand, aerodynamic noise is associated with air pumping, which produces noise above 1 *kHz* [9]. It is also related to Helmholtz resonance and tube resonators that occur in tyre cavities. On the other hand, mechanical vibrations predominate at low and medium frequencies, that is, below 1 *kHz*. These mechanisms can be further divided according to the excitation method [10]: stick–slip and stick-snap adhesion phenomena or impact phenomena caused by road irregularities.

The characteristics of the road surface also influence the acoustic emission of rolling noise, given specific parameters such as acoustic impedance [11], pavement ageing [12] or texture [13]. Research into these factors has led to the development of new types of rubberised paving and asphalts that reduce noise emission [14]. Due to all those advances, electric traction vehicles are quiet, especially at low speeds. Notwithstanding, there may still be specific situations where the noise produced by tyre-road interaction is increased due to the presence of irregularities that cause impact noise. An example of this situation is the use of speed bumps on urban roads.

1.1. Experimental research on driving over speed bumps

The effect of speed bumps on vehicles has traditionally been

* Corresponding author.
E-mail address: mfabra@umh.es (M. Fabra-Rodriguez).

https://doi.org/10.1016/j.apacoust.2023.109830
Received 11 August 2023; Received in revised form 23 November 2023; Accepted 18 December 2023
Available online 22 December 2023

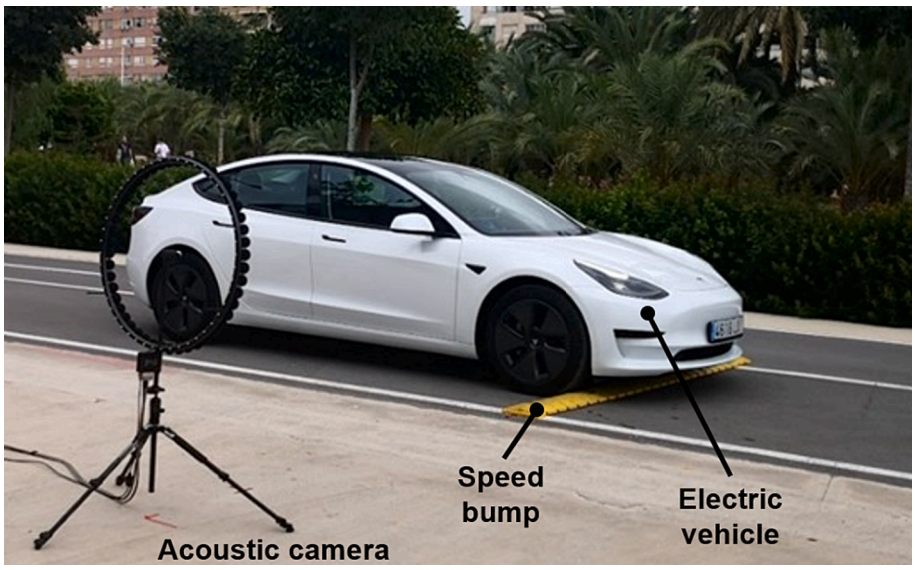

Fig. 1. Equipment used.

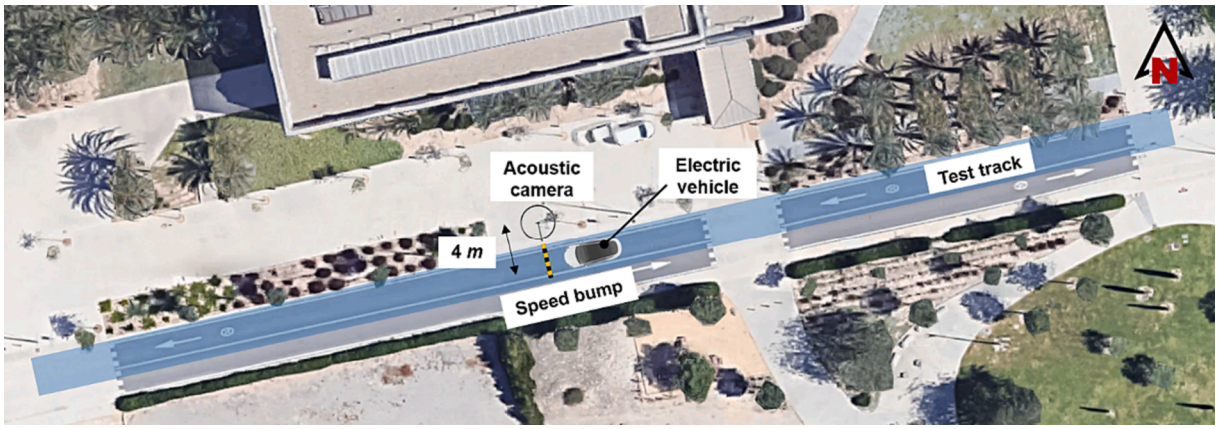

Fig. 2. Location of the tests.

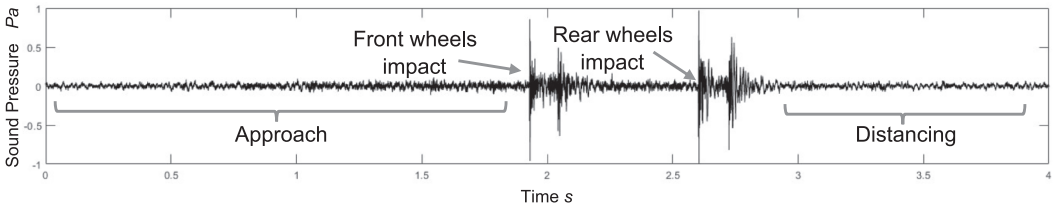

Fig. 3. Sound pressure signal recorded during a test.

investigated from a perspective focused on the analysis of internal cabin conditions. Barone *et al.* [15] developed a comfort index for driving over speed bumps based on experimental tests using a vibration dosimeter located in the driver's seat. The results concluded that, even at low speeds, speed bumps caused discomfort for vehicle occupants. On the other hand, Bilgin *et al.* [16] used experimental data obtained from an accelerometer installed under the seat, as well as finite element simulations, in order to optimise the geometry of speed bumps. In turn, Liang *et al.* [17] investigated the noise inside the cabin by tests involving driving over speed bumps using an instrumented artificial head system.

With regard to exterior noise, studies have been carried out on speed bumps in order to understand their impact on the overall production of traffic noise. Kokowski and Makarewicz [18] developed a theoretical model to predict the noise made by combustion vehicles as they pass over those devices. In their work, using the concept of energy density, they investigated the noise reduction generated by decreasing the speed of a vehicle before it reaches the speed bump, as well as the increase produced by the subsequent acceleration, but without considering the contribution of impact noise. Distefano and Leonardi [19] analysed that noise effect by varying road traffic speed in situations with multiple speed bumps in series. In this case, depending on the distances between these elements, a reduction in traffic noise was achieved due to the decrease in speed, or, conversely, there was an increase in total noise due to the successive accelerations that vehicles had to make after each speed bump to maintain a constant traffic speed.

The impact noise generated by tyres hitting speed bumps can reach

Fig. 4. Acoustic photograph at 20 *km/h*.

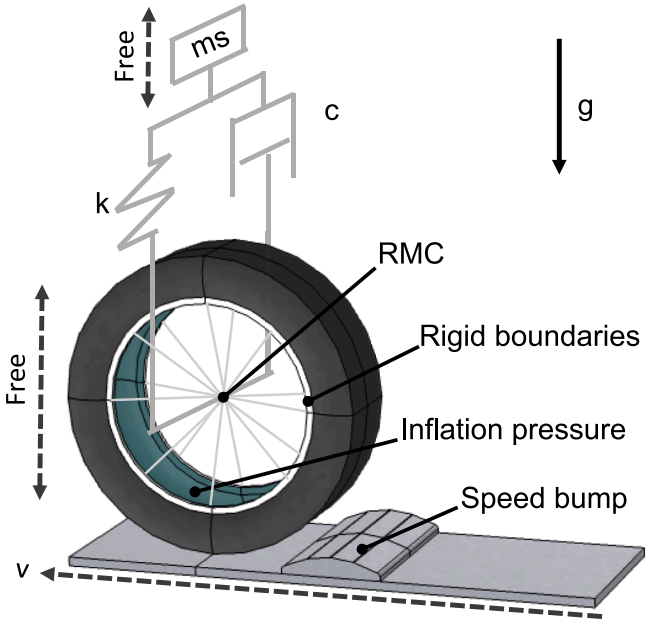

Fig. 5. Boundary conditions of the FEM analysis.

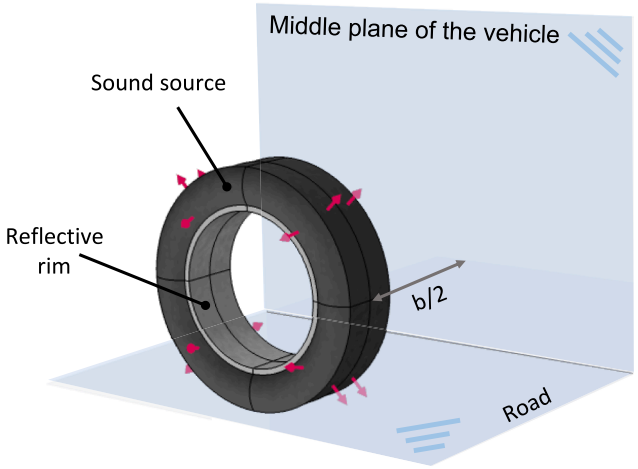

Fig. 6. Boundary conditions of the BEM analysis.

levels in excess of 90 *dB*, as recorded in the study undertaken by Janusevicius and Akelaityte [20], who used a sound level meter located 1.5 *m* from the edge of the speed bump and at a height of 1.5 *m*. Other irregularities in the road surface, such as potholes or manhole covers, also cause increases in rolling traffic noise of up to 21 *dB* [21]. Behzada *et al.* [22] modelled and experimentally investigated the sound emission of two types of speed bumps at different vehicle speeds. The tests were performed with an internal combustion vehicle, and, in order to analyse the increase in the sound level generated by going over the speed bump while isolating rolling noise, the tests were performed with the propulsion system switched off. Under these conditions, increases of up to 19 *dB* were observed at 7.5 *m* from the centre of the road and at a height of 1.2 *m*.

Table 1
Maximum sound pressure level value for each test.

Sound pressure level *dB*		Tests with speed bump				Tests without speed bump		
Speed *km/h*	Octave bands	1	2	3	Mean	1	2	Mean
5	125 *Hz* – 1 *kHz*	70.1	66.0	69.7	69.0	/	/	/
	Up to 16 *kHz*	71.5	66.9	70.3	70.0	/	/	/
10	125 *Hz* – 1 *kHz*	70.6	70.3	72.3	71.1	57.4	59.2	58.4
	Up to 16 *kHz*	71.5	71.6	73.4	72.3	62.0	61.4	61.7
15	125 *Hz* – 1 *kHz*	74.1	72.6	75.5	74.2	/	/	/
	Up to 16 *kHz*	74.8	74.3	76.2	75.2	/	/	/
20	125 *Hz* – 1 *kHz*	78.8	75.1	76.3	77.0	58.5	62.2	60.8
	Up to 16 *kHz*	79.8	76.2	77.5	78.1	59.8	62.9	61.6

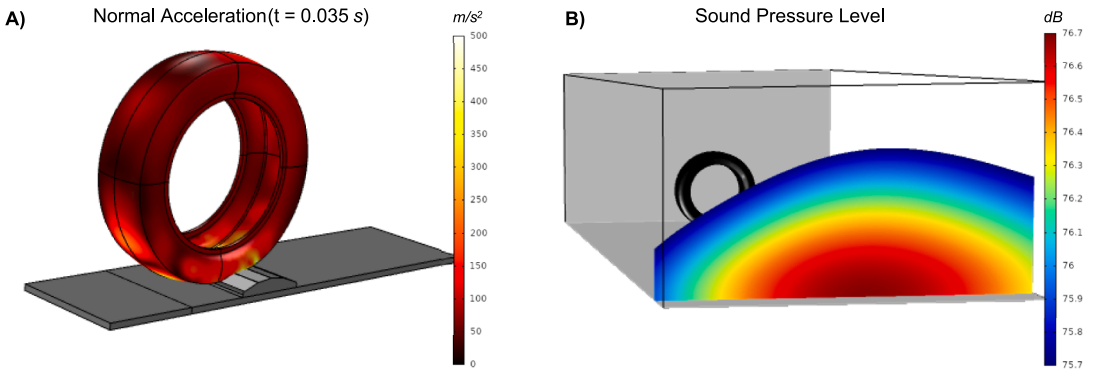

Fig. 7. Simulations at 20 *km/h*: A) Frame of the dynamic analysis B) Result of the propagation analysis.

Table 2
Maximum value of the simulated sound pressure level.

Speed, *km/h*	5	10	15	20
Sound pressure level, *dB*	68.0	71.0	74.6	78.1

1.2. Numerical modelling of rolling noise

With regard to models that enable tyre-road interaction noise to be studied, these are classified according to the literature [23] as statistical and deterministic. Statistical models are fed by large databases obtained from experimental measurements to develop prediction models through regressions. One example of these models is CNOSSOS (Common Noise Assessment Methods in Europe) [24], which is currently used for developing noise maps in the member countries of the European Union. Deterministic models, on the other hand, focus on the study of specific generation mechanisms, e.g., air pumping [25] or vibrations [26]. These are divided into analytical or numerical models.

Among the deterministic models, the numerical finite element method (FEM) has been used to analyse the propagation of tyre-road interaction. Lafon *et al.* [27] used a statistical model to compare the sound propagation obtained from a tyre and from a simplification of monopole sources. In that study, the road surface was modelled as a rigid, reflective surface, while the absorption condition at infinity was achieved by using the *Perfectly Matched Layers* boundary condition. On the other hand, Biermann *et al.* [28] used the Boundary Element Method (BEM), which enables sound absorption conditions at infinity to be simulated in order to study the sound radiation from tyres under rolling conditions. The advantage of this method is that it does not need to discretise air volume, as it is computationally more efficient to evaluate sound propagation in large open spaces.

Regarding the numerical models used to predict impact noise, Behzada *et al.* [22] used a two-degree-of-freedom, lumped quarter-vehicle model to obtain the force acting on a tyre as it passes over a speed bump. The resulting force was then used to develop a 3D FEM analysis to study the sound pressure level achieved. The tyre-assembly can also be modelled directly in 3D, as presented by Han *et al.* [29], where they simulated the passage of a tyre over a bar where the normal acceleration of its surface is used as a sound source.

In the work presented in this paper, a numerical model is proposed to analyse the sound produced by a tyre when it interacts with speed bumps on the road. The model consists of two steps; firstly, a dynamic analysis is performed using FEM of a quarter-vehicle model to study the vibration produced on the tyre surface. That vibration is then used as a sound source in an acoustic propagation analysis using BEM. The model is based on the development initiated by the authors in [30] where the impact noise of a tyre against a flat surface was studied.

In order to validate the model developed, low-speed driving tests using an electric vehicle and a speed bump were carried out. In these tests, an acoustic camera was used, which enables the acoustic signal to be recorded and the sound field to be visualised.

2. Experimental methodology

2.1. Equipment

The equipment used to carry out the tests consists of an electrically propelled passenger car, a speed bump and an acoustic camera as a measuring instrument. The general layout of the test is shown in Fig. 1.

The acoustic camera used is the *Array Ring48 AC Pro* model, with 48 microphones in a circular array arrangement with a diameter of 75 *cm*, which enables the behaviour of sound waves in a given space to be mapped and displayed. It has a video camera in the centre of the array, which enables the sound field superimposed on the filmed digital image to be displayed.

The electric vehicle used for the tests is a 2022 *Tesla Model 3 Standard Plus RWD*, a version with a single motor on the rear axle. This vehicle is fitted with ISO code [31] *235/45* R18 tyres that were inflated to a pressure of 2.2 *bar*. By using a vehicle scale, it was determined that the mass resting on each wheel of the front axle is 500 *kg* while the weight of each rim is 13 *kg*. The vehicle has a factory fitted acoustic alert system which, according to the latest revisions to the regulations [32], cannot be disconnected, so the audible alert remained active during the tests.

The speed bump is made of a rigid plastic material and is of a transportable type to be used in traffic controls or interventions where

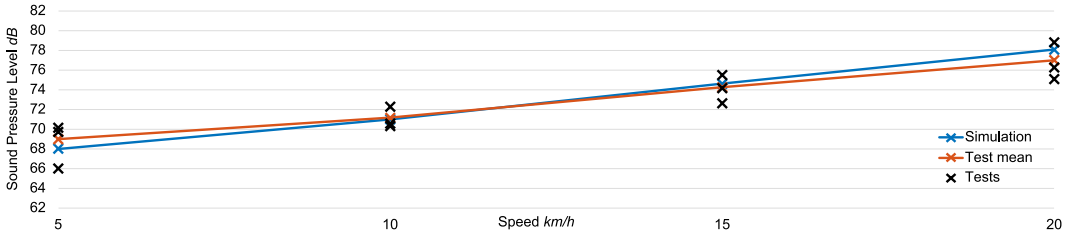

Fig. 8. Comparison between the numerical and experimental data.

traffic is limited. The speed bump has a cross-sectional width of 225 *mm* and a maximum height of 45 *mm*.

2.2. Tests

The tests were performed at the facilities of the Miguel Hernández University of Elche. An interior track, closed to traffic, 120 *m* in length, was provided. Fig. 2 shows the location of the test track on which the speed bump was located. The acoustic camera was positioned in line with the speed bump, at a height of 1.2 *m* and at a distance of 4 *m* from the centre of the track.

The tests were performed at constant speed at 5, 10, 15 and 20 *km/h* with three repetitions for each of the speeds in the study. Higher speeds were not achieved for safety reasons due to the severity of the impacts. The passage of the electric vehicle was also recorded at 10 and 20 *km/h* while driving on the track without a speed bump.

2.3. Processing

Both acquisition and post-processing were performed using *Noise Image* software, which works in conjunction with the acoustic camera. To record each test, a signal of 4 *s* duration was captured, with 2 *s* before and 2 *s* after the vehicle passed over the speed bump. That signal was acquired for each of the 48 microphones of the array at a sampling frequency of 96 *kHz*. Fig. 3 shows the sound pressure corresponding to one of the microphones during the performance of one of the tests, where it can be seen when the passage over the speed bump occurs for each axle of the electric vehicle.

In the subsequent processing, a time window is selected in the sound pressure signal to generate the corresponding acoustic photograph by combining the information from all the microphones in the array. In this study, a time window of 0.125 *s*, the value of the *fast* time weighting, was established, from the moment the front wheels hit the speed bump. The acoustic photographs are generated to cover the frequency range to be studied. Fig. 4 shows an example of the acoustic photograph obtained for one of the tests at 20 *km/h* in the octave band range from 125 to 1000 *Hz*, both included. The sound pressure level shown in Fig. 4 is the acoustic field equivalent to the time window in the vertical plane of the camera position. The colour scale has been plotted from the maximum sound pressure level of the array plane in a 1 *dB* descending range.

3. Numerical modelling

The model is divided into two parts, the first corresponds to the dynamic simulation in the time domain of a quarter vehicle using FEM and the second part corresponds to the acoustic simulation in the frequency domain using BEM. The entire model has been implemented using *COMSOL Multiphysics* software.

3.1. Dynamic simulation

The proposed FEM model of a quarter vehicle consists of a 3D tyre connected to the suspended mass *ms* by means of the spring of rigidity *k* and the damper of coefficient *c*. The tyre is represented as a linear elastic solid with different material properties for each of its component parts. The tyre geometry is parameterised to be generated from the ISO code [31] that defines its size. The details of the mesh, as well as the material property values can be consulted in [30], where the tyre was considered as an element isolated from the rest of the vehicle. The tyre and the suspended mass are free to move vertically, while the road surface, which includes the speed bump, is modelled as a rigid solid moving horizontally at the driving speed *v*. Tyre does not rotate during simulation whereas a frictionless contact condition is defined between the tyre tread and the road surface to reproduce the impact.

The boundary conditions of the system are shown schematically in Fig. 5. The tyre is subjected to an inflation pressure applied as a force per unit area normal to its inner surface. The rim is modelled by stiffening the contours of the bead that would be in contact with it. On these contours, the weight of the rim is applied as an aggregate point mass at its centre of gravity, named *RMC*. This centre of mass is also used to serve as a connection to the force transmitted by the suspension system. The gravity acceleration affects the whole model.

When running the simulations, a preliminary stationary step is carried out so that the tyre acquires the initial deformation, the tyre contact path is generated and the vertical equilibrium of the suspension system is reached. The transitory analysis of the impact of the tyre on the speed bump is then carried out.

3.2. Simulation of acoustic propagation

After the dynamic analysis, the Fast Fourier Test (FFT) is applied to the acceleration field $\ddot{u}$ of the tyre surface during a limited time window. In this way, the tyre vibration is related to the sound pressure p in the frequency domain according to Equation (1), where n is the unit vector normal to the surface and ρ is the density of the medium.

$$-n\cdot\left(-\frac{1}{\rho}\nabla p\right)=n\cdot\ddot{u} \tag{1}$$

The boundary conditions of the BEM model are shown in Fig. 6. The tyre geometry acts as a sound source. The vibration acceleration obtained in the previous dynamic analysis is mapped onto the outer surface of the tyre geometry, in a configuration without deformation due to vehicle weight. The rim is now modelled as a reflective surface and two reflective planes are added. The horizontal plane represents the road surface. The vertical plane, located at a distance from the centre of the tyre equal to half the track width *b* of the vehicle, acts as symmetry along the longitudinal median plane of the vehicle. Therefore, the sound contribution of the tyre in parallel to that of the quarter-vehicle model under study is also considered, resulting in a half-vehicle sound prediction model.

The acoustic analysis is performed in a stationary manner for each discrete frequency of the desired range. For this purpose, a sweep study is performed where the increment between the study frequencies is the inverse of the duration of the time window.

4. Results

4.1. Experimental results

Table 1 shows the maximum sound pressure level values recorded in the plane of the acoustic camera for each test performed. These values are obtained both for the frequency range covering the octave bands from 125 to 1000 *Hz* and for the entire sound spectrum, including up to the 16 *kHz* band. The background noise did not exceed 55 *dB* during the tests.

The differences in sound pressure level between the tests are due to the difficulty in keeping the vehicle speed stable before and during the impact, as the vehicle speed control does not work for the low driving speeds tested. The mean results were calculated as the logarithmic mean of the tests performed at the same speed. In the tests over speed bumps, the difference in levels between frequency ranges oscillates between 0.6 and 1.7 *dB*, which shows that the phenomenon of rolling noise generation studied in the impact is predominant below 1 *kHz*.

Among the mean values, for the range from 125 to 1000 *Hz*, passing over the speed bump at 10 *km/h* represents an increase of 12.7 *dB* with respect to normal rolling without obstacles. At 20 *km/h*, this difference is even more pronounced and reaches 16.2 *dB*. At 10 *km/h*, in the test without speed bumps, there are greater differences between the two frequency ranges, which is due to the acoustic warning system that remains active during tests. On the other hand, at 20 *km/h*, the acoustic warning system is dulled by the rolling noise.

4.2. Numerical results

The simulations were run by replicating the test conditions. The modelled tyre has the dimensions and inflation pressure of those of the *Tesla Model 3,* and the geometry of the speed bump was profiled. The mass of the quarter vehicle *ms* and the weight of the rim are set to the measured values.

Regarding the data for the suspension system, the damping coefficient *c* was set to the usual value of 3000 *N s/m* according to the literature [33]. The stiffness value *k* is obtained theoretically according to the simplified design method for suspensions [34]. This method fixes the natural frequency of a one-degree-of-freedom spring-mass system at 1 *Hz*, as shown in equation (2), from which a *k* value of 19,739.2 *N/m* is obtained, which has been approximated to 20,000 *N/m*.

$$k = 4\pi^2 ms \tag{2}$$

The dynamic FEM simulations were performed at speeds *v* of 5, 10, 15 and 20 *km/h*, obtaining the results with a frequency of 3000 *Hz*. Fig. 7.A shows a frame of the dynamic simulation at 20 *km/h*. The normal acceleration of the tyre's outer surface was plotted on the tyre.

After each dynamic analysis, a time window of 0.125 *s*, equivalent to that used in the experimental methodology, is established from the instant at which contact between the tyre and the speed bump occurs. For this limited time fragment, the FFT of the normal acceleration of the tyre surface is performed, which is later used as the sound source in the BEM propagation analysis.

For the BEM propagation analysis, the distance between the centre of the tyre and the reflective vertical plane is 1.58 *m*, which is half the track width of the vehicle. The sound analyses are performed in increments of 8 *Hz*, inverse to the time window, from the frequency of 88 *Hz* to 1408 *Hz*. In this way, the sound contribution of the octave bands from 125 to 1000 *Hz* is covered. Fig. 7.B shows the sound pressure level obtained as the logarithmic sum of each discrete frequency being studied, plotted in the vertical plane whose distance to the reflective plane is 4 *m*, equivalent to that of the acoustic camera.

Table 2 shows the maximum sound pressure level values of the numerical analyses achieved in the vertical plane equivalent to the acoustic camera for each of the speeds studied in the BEM simulation.

4.3. Validation

The comparison between the experimental and numerical results are shown in Fig. 8. The comparison is made with the experimental data covering the frequency range of the octave bands from 125 to 1000 *Hz*.

The results provided by the simulation are within the range marked by the experimental results. The model displays a behaviour close to the mean line of the experimental results, with a slope of 0.5 *dB* per *km/h* for the mean of the tests and 0.7 *dB* per *km/h* for the numerical results. The maximum difference between the model and the experimental mean is 1.1 *dB* at 20 *km/h*.

5. Conclusions

In this work, a numerical model combining FEM and BEM has been developed, which allows the study of the impact noise produced by a vehicle passing over speed bumps in the. The model consists of a first dynamic analysis of a quarter vehicle in which aspects such as the tyre geometry, the value of the suspension and driving speed, among others, are specified. The subsequent sound analysis enables the sound propagation of the noise generated by the vibration of the tyre surface to be determined. The model has limitations, notably, it does not take into account the effect of the air inside the tyre cavity, and it does not provide the acoustic results in a transient mode.

To check the correct functioning of the model, driving tests were carried out on a track with an electric vehicle going over a speed bump. An acoustic camera has been used to visualise and locate the source of the noise, as well as to determine its magnitude. The experimental results also show the increase in the sound level produced when driving over a speed bump compared to driving without obstacles, reaching increases of up to 13 *dB* when driving at 10 *km/h*, and more than 16 *dB* at 20 *km/h*.

The validation of the model was undertaken by comparing the maximum sound pressure level values obtained in the plane of the acoustic camera with those of the simulations carried out under experimental conditions. The results of the validation confirm the correct functioning of the model, obtaining a maximum difference between the model and the mean of the 1.1 *dB* test results at 20 *km/h*.

As a future line of work, the use of the model as a design tool for speed bumps is proposed to try to mitigate the noise pollution they produce in their environment. The acoustic impact of other types of irregularities, such as potholes, can also be studied in order to analyse the sound behaviour of roads in poor condition. Another approach currently being worked on consists of using the sound prediction model developed to study various proposals for road surface elements, such as rumble strips, which can be used as an acoustic warning element external to the vehicle in areas of particular danger to pedestrians.

CRediT authorship contribution statement

Miguel Fabra-Rodriguez: Methodology, Software, Writing – original draft. **David Abellán-López:** Investigation, Software, Writing – review & editing. **Francisco J. Simón-Portillo:** . **Hector Campello-Vicente:** Validation, Resources. **Nuria Campillo-Davo:** Formal analysis, Writing – review & editing. **Ramon Peral-Orts:** Conceptualization, Supervision.

Declaration of competing interest

The authors declare that they have no known competing financial interests or personal relationships that could have appeared to influence the work reported in this paper.

Data availability

The data that has been used is confidential.

Acknowledgements

This work has received a Research Project Grant, from the Call for Research Grants of the UMH Vice-Rectorate for Research, call 2023. In addition, the authors would like to thank gfai tech GmbH for providing the measuring equipment.

References

[1] European Environment Agency, Environmental noise in Europe 2020, EEA Report 22/2019.
[2] Muzet M. Environmental noise, sleep and health. Sleep Med Rev 2007;11(2):135–42.
[3] Skrzypek M, Kowalska M, Czech EM, Niewiadomska E, Zejda JE. Impact of road traffic noise on sleep disturbances and attention disorders amongst school children living in Upper Silesian Industrial Zone, Poland. Int J Occup Med Environ Health 2017;30(3):511–20.
[4] Babisch W, Swart W, Houthuijs D, Selander J, Bluhm G, Pershagen G, et al. Exposure modifiers of the relationships of transportation noise with high blood pressure and noise annoyance. J Acoust Soc Am 2012;132(6):3788–808.
[5] Nelson P. Transportation Noise Reference Book. Butterworths-Heinemann 1987.
[6] Sandberg U, Ejsmont JA. Tyre/road noise reference book. Kisa, Sweden: Informex; 2002.
[7] Sancho S, Gaja E, Peral-Orts R, Clemente G, Sanz J, Velasco-Sánchez E. Analysis of sound level emitted by vehicle regarding age. Appl Acoust 2017;126:162–9.
[8] Campello-Vicente H, Peral-Orts R, Campillo-Davo N, Velasco-Sanchez E. The effect of electric vehicles on urban noise maps. Appl Acoust 2017;116:59–64.
[9] Morgan PA, Phillips SM, Watts GR. The localisation, quantification and propagation of noise from a rolling tyre. TRL Limited 2007.

[10] Kuijpers A, Van Blokland G. In: Tyre/road noise models in the last two decades: a critical evaluation. The Hague; 2001. p. 2494–9.
[11] F. Bianco L. Fredianelli F. Lo Castro P. Gagliardi F. Fidecaro G. Licitra Stabilization of a p-u sensor mounted on a vehicle for measuring the acoustic impedance of road surfaces Sensors 20 5 1239. 2020.
[12] Luca T, de León G, Del Pizzo LG, Moro A, Bianco F, Fredianelli L, et al. Modelling the acoustic performance of newly laid low-noise pavements. Constr Build Mater 2020;247:118509.
[13] Del Pizzo A, Teti L, Moro A, Bianco F, Fredianelli L, Licitra G. Influence of texture on tyre road noise spectra in rubberized pavements. Appl Acoust 2020;159:107080.
[14] de León G, Del Pizzo LG, Teti L, Licitra G. Evaluation of tyre/road noise and texture interaction on rubberised and conventional pavements using CPX and profiling measurements. Road Mater Pavement Des 2020;21(sup1):S91–102.
[15] Barone V, Mongelli D, Tassitani A. Vibrational comfort on board the vehicle: influence of speed bumps and comparison between different categories of vehicle. Adv Acoust Vibration 2016;2016(13):1–6.
[16] Bilgin E, Hilmi Lav A, Gedik A. An approach for the determination of optimal speed hump/table profiles by field tests and simulation stage. Sustain Cities Soc 2019;51:101716.
[17] Liang L, Chen S, Li P. The evaluation of vehicle interior impact noise inducing by speed bumps based on multi-features combination and support vector machine. Appl Acoust 2020;163(16):107212.
[18] Kokowski P, Makarewicz R. Predicted effects of a speed bump on light vehicle noise. Appl Acoust 2006;67(6):570–9.
[19] Distefano N, Leonardi S. Experimental investigation of the effect of speed bumps in sequence on noise emission level from motor vehicles. Noise Control Eng J 2015;63(6):582–97.
[20] Janusevicius T, Akelaityte R. Speed bumps impact on motor transport noise. The Baltic J Road Bridge Eng 2015;10(2):191–9.
[21] Cantisani G, Fascinelli G, Loprencipe G. Urban Road Noise: The Contribution of Pavement Discontinuities. Texas: and Construction; 2012.
[22] Behzada M, Hodaeia M, Alimohammadib I. Experimental and numerical investigation of the effect of a speed bump on car noise emission level. Appl Acoust 2017;68(11–12):1346–56.
[23] Li T, Burdisso R, Sandu C. Literature review of models on tire-pavement interaction noise. J Sound Vib 2018;420:357–445.
[24] Joint Research Centre, Common Noise Assessment Methods in Europe (CNOSSoS-EU), Report EUR 25379, 2012.
[25] Leba-Bassil MB, Cesbrond J, Klein P. Tyre/road noise: A piston approach for CFD modeling of air volume variation in a cylindrical road cavity. J Sound Vib 2020;469:115140.
[26] McBride S, Burdisso R, Sandu C. Modeling vibration-induced tire-pavement interaction noise in the mid-frequency range. Tire Sci Technol 2021;49(2):146–69.
[27] Lafont, T.; Stelzer, R.; D'amico, R.; Bertolini, C.; Kropp, W. Modeling Tyre Noise in FE Simulations for Pass-By Noise Predictions. Conference: Noise and Vibration Emerging Methods, Auckland (2018).
[28] Biermann J, Estorff O, Petersen S, Schmidt H. Computational model to investigate the sound radiation from rolling tires. Tire Science and Technology 2007;35(3).
[29] Han M, Lee C, Park T. Vibro-acoustic response in vehicle interior and exterior using multibody dynamic systems due to cleat impacts. Int J Automot Technol 2020;21(3):591–602.
[30] Fabra-Rodriguez M, Peral-Orts R, Abellán-López D, Campello-Vicente H, Campillo-Davo N. Numerical sound prediction model to study tyre impact noise. Appl Acoust 2023;206:109325.
[31] ISO 4000-1:2015, Passenger car tyres and rims - Part 1: Tyres (metric series).
[32] Official Journal of the European Union, Regulation No 138, Uniform provisions concerning the approval of Quiet Road Transport Vehicles with regard to their reduced audibility, 2017.
[33] Mehmood A, Ali Khan A, Mehmood A. Optimization of suspension damping using different mathematical car models. Int J Mech Eng 2013;3(10):1–15.
[34] Gillespie TG. Fundamentals of vehicle dynamics. SAE Int 1992.